Layer coupling and read disturbances in a buffered magnetic logic environment

Thomas Windbacher, Alexander Makarov, Viktor Sverdlov, and Siegfried Selberherr[a]

[a]Institute for Microelectronics, TU Wien, Gußhausstraße 27-29/E360, Vienna, Austria

Keywords: spin-transfer torque, flip flop, non-volatile, majority gate, read disturbance, layer coupling, stray field, reliability

ABSTRACT

There are two major obstacles impeding computing systems from further advancements: The power dissipation due to leakage and the energy spent for the information transfer between memory and processor(s). The first issue is commonly handled by shutting down unused circuit parts, however, when the dormant circuits are turned on again, their previous state must be recovered. This is commonly realized by retrieving the required information from the memory, which exacerbates the limited bandwidth between memory and processor(s). In order to circumvent these limitations, we have proposed a non-volatile buffered magnetic logic grid with instant-on capability. Non-volatile magnetic flip flops and spin-transfer torque majority gates are combined to a compact regular structure, which enables a small layout foot print as well as it guarantees the reduction of the information transfer due to a shared buffer. In the proposed structure the information is passed from one magnetic layer to another by first running a current through the magnetic layer to be read, which subsequently generates a magnetization orientation encoded spin-transfer torque, when the polarized electron spins enter the next layer. Since the current passing through the junction also exerts a spin-transfer torque on the read layer, its magnetization orientation could be destabilized which might cause a read disturbance. However, during our simulations it was also found out that the stray fields of neighboring layers have a non-negligible influence on the proposed copy operation. In this work we investigate these potential read disturbances in detail for a 2-bit shift register for varying stray field strength by changing the thickness of the interconnection layer. We found that for closer proximity the acting stray fields not only stabilize but also speed up the copy procedure, while for increasing interconnection layer thickness oscillating domain walls are formed and the copy operation becomes unreliable.

1. INTRODUCTION

Over the years many tough problems obstructing the way to further progress in CMOS technology have been resolved. Nevertheless, for each new technology generation new and ever harder obstacles appear and, in conjunction with the soaring manufacturing costs, further progress in CMOS technology will come to a halt in the near future. For instance, two of the currently most performance limiting bottlenecks, among the multitude of challenges in CMOS technology, are the power dissipation due to leakage and the energy spent for the continuous information transport between the physically separated memory and processors.[1,2] In order to get rid of the power dissipated by leakage, unused circuit parts are commonly entirely shut down. Despite the fact that the dissipated power in these circuit parts is reduced to zero, it also causes the loss of the information stored in the circuit due to leakage. Therefore, every time the circuit is activated all lost information must be recovered before it actually can start with its operation. This is usually done by copying the data back from memory, which degrades the already strained bandwidth between memory and processors further. In order to avoid this shortcoming one has to introduce non-volatile elements into the circuits close to the combinational logic. Spintronics offers such non-volatile devices and fits very well into the needs for this type of application. These spintronic devices are CMOS compatible, non-volatile, exhibit high endurance, and fast operation.[3] Since the term spintronics is rather broad in its use, there is a vast diversity of ideas for devices and operation principles.[3,4]

http://www.iue.tuwien.ac.at, E-mail:{windbacher|makarov|sverdlov|selberherr}@iue.tuwien.ac.at

Spintronics IX, edited by Henri-Jean Drouhin, Jean-Eric Wegrowe, Manijeh Razeghi, Proc. of SPIE
Vol. 9931, 99312M · © 2016 SPIE · CCC code: 0277-786X/16/$18 · doi: 10.1117/12.2236151

For our work we focused on ideas with prospects for near to mid term realization in large scale applications. Here, the combination of spintronic and CMOS technology to hybrid solutions are - in our opinion - very promising. Indeed, the combination of CMOS technology with magnetic tunnel junctions (MTJ) led already to first commercial stand-alone magneto resistive random access memory (MRAM) and embedded DRAM,[5] and additional innovative commercial products will surely follow soon.[1,6–8]

The key for the success of the before mentioned MRAM is the all-electrical magnetization manipulation by spin-transfer torque (STT),[9] which allows to avoid of the formerly required wires for the switching field generation and also significantly reduces the MTJ switching energy. Additional improvements like the transition to free layers with perpendicular magnetic anisotropy and the use of MgO tunnel barriers brought advances in the reduction of the switching energy and improved scalability further.[10]

Even though also first non-volatile solutions for logic already exist and they are competitive in comparison to pure CMOS with respect to speed and power consumption, their integration density - one of the keys of CMOS technologies success - can not compete. The reason is that these CMOS/MTJ hybrid structures employ MTJs only as auxiliary storage, while the actual computation is still carried out via CMOS logic. The introduction of the MTJs also increases the circuit complexity and the footprint, since extra transistors are required to access and write the data stored in the MTJs.[1,11]

This observation encouraged us to push as much as possible functionality into the magnetic domain, which led to the proposal of a non-volatile magnetic flip flop (cf. Fig. 1)[12] and a nano-scale spin-transfer torque oscillator[13] as well as circuits employing them such as a non-volatile magnetic shift register[14] (see Fig. 2) and a non-volatile buffered magnetic logic grid (see Fig. 3 and Fig. 4).[15] All these components are essential for building a buffered magnetic logic environment for non-volatile computation. Due to consequent avoidance of signal conversion between the magnetic and the CMOS domain in combination with the non-volatile information storage in the shared free magnetic layers, the proposed circuits feature instant-on capabilites, a very small layout footprint, a highly regular structure, and a considerable decrease in the actual information transport.[12,15,16]

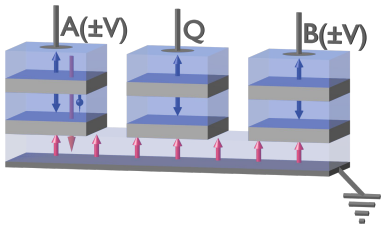

Figure 1: The non-volatile magnetic flip flop consists of three synthetic anti-ferromagnetic polarizer stacks with out-of-plane magnetization orientation. The polarizer stacks A and B are dedicated to inputs, while the stack Q is used for readout. The polarizer stacks share a common free magnetic layer with a uniaxial out-of-plane anisotropy via non-magnetic interconnection layers.

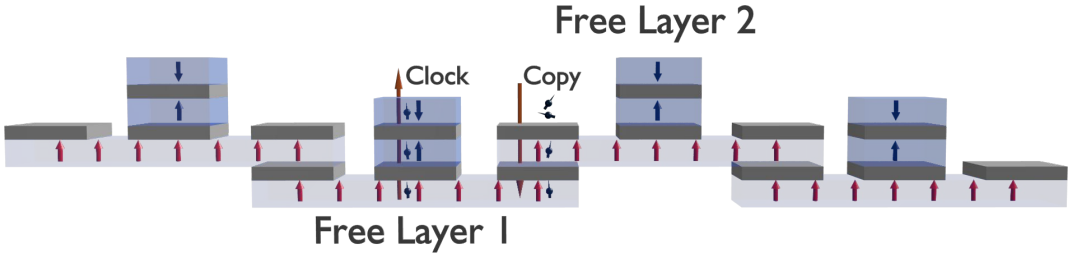

Figure 2: The non-volatile shift register comprises two rows of overlapping non-volatile flip flops in two distinct levels. Each flip flop on one level is connected at its ends to two flip flops in the respective other level. The polarizer stacks in the middle of the free layers are used to generate a second clocked auxiliary spin-transfer torque contribution during the copy procedure.

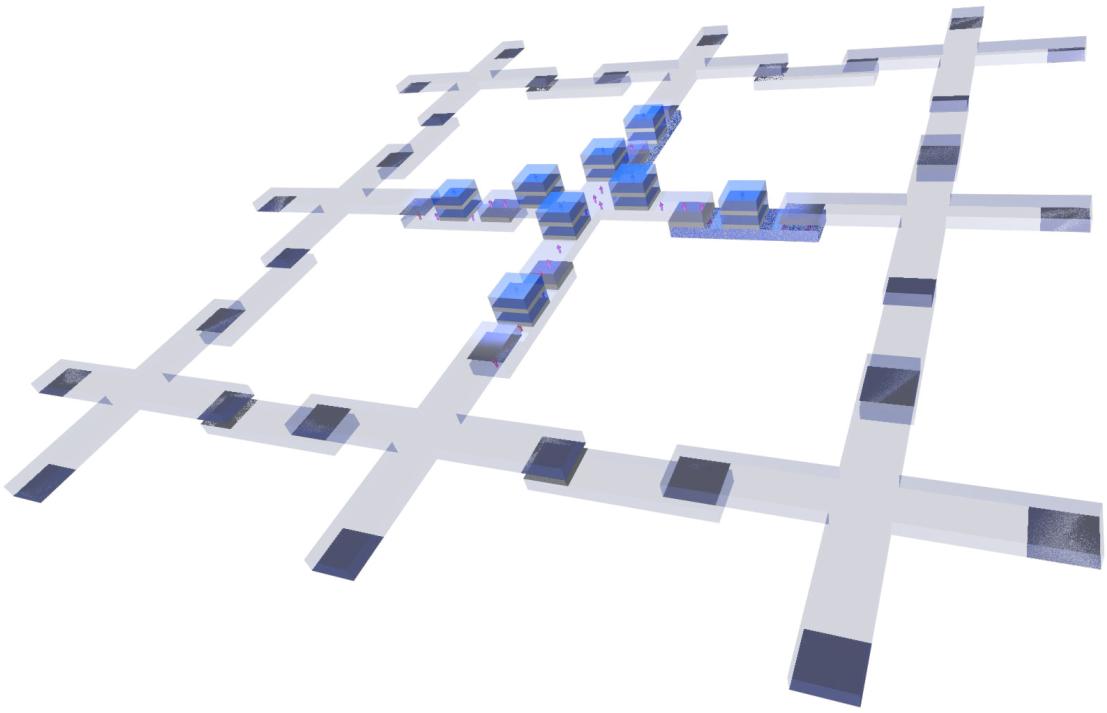

Figure 3: For the proposed non-volatile buffered logic gate grid the spin-transfer torque majority gates (crosses) perform the logic operations and the adjacent non-volatile flip flops (rectangles) act as shared buffers.

Nevertheless, still one has to be able to transport information from one device to another. Therefore, we proposed to copy information from one free layer to an adjacent free layer (cf. Fig. 2 and Fig. 4) by pushing a current through the read layer to generate a magnetization orientation encoded spin polarized current. When this spin polarized current enters the neighboring layer, it exerts a spin-transfer torque on the local magnetization, which enables copying the magnetization state from the previous layer.

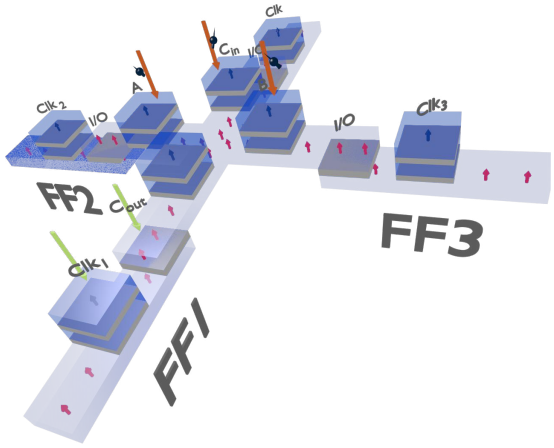

Figure 4: Already a single majority gate and three flip flops are sufficient to realize a concatenable non-volatile 1-bit full adder.[15]

However, since the read layer also experiences a torque, when the passing electrons are polarized, there is the potential risk of flipping the magnetization, which would cause a read error. To avoid such read errors, we came up with the idea to add a second spin-transfer torque contribution which acts on the written layer to speed up

the write procedure and to reduce the magnetization excitation of the read layer. Recently, we could show via extensive micro magnetic simulations that the proposed operation indeed is capable of avoiding read errors.[17] But we also observed that the stray fields in the overlapping layer regions are so strong that they could cause errors during the copy operation as well. Therefore, we study in this work the copy procedure with respect to different free layer spacings in order to analyze the influence of the stray field strength on the reliability of the copy operation.

2. THEORY

Before going into the details of the simulation setup, it is necessary to elucidate the employed models and how they incorporate the acting physical effects on the free layers. The dynamics of the studied magnetic devices is described by the Landau-Lifshitz-Gilbert equation[18,19] and the effect of the spin-transfer torques is taken care off by the additional spin-transfer torque terms $\vec{T}_{\text{clock}}$, $\vec{T}_1$, and $\vec{T}_2$:

$$\frac{\mathrm{d}}{\mathrm{d}t}\vec{m} = \gamma\left(-\vec{m}\times\vec{H}_{\text{eff}} + \alpha\left(\vec{m}\times\frac{\mathrm{d}}{\mathrm{d}t}\vec{m}\right) + \vec{T}_{\text{clock}} + \vec{T}_1 + \vec{T}_2\right) \tag{1}$$

$\vec{m}$ denotes the reduced magnetization, γ the electron gyromagnetic ratio, α the dimensionless damping constant, and $\vec{H}_{\text{eff}}$ incorporates the effective field. $\vec{H}_{\text{eff}}$ is given by the functional derivative of the free energy density and incorporates energy contributions from the uni-axial anisotropy, exchange, demagnetization, and thermal excitations[20] in a straight forward manner.

The effective field $\vec{H}_{\text{eff}}$ drives precessional motions which are covered by the first term in (1). The second term introduces a power dissipation proportional to $\frac{\mathrm{d}}{\mathrm{d}t}\vec{m}$ and the last three terms describe the spin-transfer torques acting on the read and the written free layer.

If one assumes that the non-magnetic interconnecting layers are made out of copper (spin valve stack), the strength and angle dependence of the acting torques can be described by a model from Xiao et al.[21] Assuming further that the energy required to switch the magnetization of the polarizer stack used for creating the auxiliary clocked spin-transfer torque is much higher than the switching energy of the free layers, their magnetization will not change during operation and therefore it is save to assume that the unit polarization direction $\vec{p}$ is constant during the copy operation. Thus the auxiliary spin-transfer torque contributions $\vec{T}_{\text{clock}}$ can be written as:

$$\vec{T}_{\text{clock}} = \frac{\hbar}{\mu_0 e}\frac{J_{\text{clock}}}{l_1 M_S}\frac{P\Lambda^2}{(\Lambda^2+1)+(\Lambda^2-1)\,\vec{m}_1\cdot\vec{p}}\cdot \\ \cdot\,(\vec{m}_1\times\vec{p}\times\vec{m}_1 + \epsilon'\vec{m}_1\times\vec{p}) \tag{2}$$

$\hbar$ denotes the Planck constant, μ_0 the magnetic permeability, J_{clock} the applied current density, l_1 the thickness of the written Free Layer 1 (see Fig. 2), M_S the magnetization saturation, P the spin current polarization, $\vec{p}$ the unit polarization direction of the polarized current, and Λ a fitting parameter handling the contact geometry. Furthermore, the spin-transfer torque model for spin valves features an in-plane $(\vec{m}_1\times\vec{p}\times\vec{m}_1)$ and a small out-of-plane torque contribution $(\vec{m}_1\times\vec{p})$.[22]

The second spin-transfer torque $\vec{T}_1$ is created by the spin valve structure formed in the regions where two free layers overlap (see Fig. 2 and Fig. 4). Since also here a copper interface was chosen, the model from Xiao[21] is applicable and it is sufficient to simply exchange the unit polarization vector $\vec{p}$ with the magnetization orientation $\vec{m}_2$ of the neighboring Free Layer 2:[23]

$$\vec{T}_1 = \frac{\hbar}{\mu_0 e}\frac{J_{\text{copy}}}{l_1 M_S}\frac{P_1\Lambda_1^2}{(\Lambda_1^2+1)+(\Lambda_1^2-1)\,\vec{m}_1\cdot\vec{m}_2}\cdot \\ \cdot\,(\vec{m}_1\times\vec{m}_2\times\vec{m}_1 + \epsilon_1'\vec{m}_1\times\vec{m}_2) \tag{3}$$

J_{copy} denotes the applied current density, P_1 describes the spin current polarization, Λ_1 the fitting parameter for non-idealities, and ϵ'_1 the out-of-plane torque strength for Free Layer 1 in the overlapping region.

Finally, the third spin-transfer torque $\vec{T}_2$ is created in the overlapping regions, when the unpolarized electrons enter Free Layer 2 and align to the local magnetization orientation. Also here the model from Xiao et al.[21] can be employed, since Free Layer 2 shares the copper interface with Free Layer 1. Due to symmetry reasons the torque acts in the opposite direction of $\vec{T}_1$ and the unit polarization direction is described by the reduced magnetization orientation $\vec{m}_1$:[23]

$$\vec{T}_2 = -\frac{\hbar}{\mu_0 e}\frac{J_{\mathrm{copy}}}{l_2 M_S}\frac{P_2\Lambda_2^2}{(\Lambda_2^2+1)+(\Lambda_2^2-1)\,\vec{m}_2\cdot\vec{m}_1}\cdot \\ \cdot\,(\vec{m}_2\times\vec{m}_1\times\vec{m}_2+\epsilon'_2\vec{m}_2\times\vec{m}_1) \tag{4}$$

Since the whole current which enters in the overlapping region into Free Layer 2 is passed over to Free Layer 1, the applied current density J_{copy} is the same for both layers. l_2 describes the free layers' thickness, P_2 denotes the spin current polarization, Λ_2 the fitting parameter for non-idealities, and ϵ'_2 the out-of-plane torque strength in the overlapping region of Free Layer 2.

3. SIMULATION SETUP

To be able to incorporate all governing physical effects and keep the required amount of combinations to study reasonable, we restricted our analysis to a shift register with two flip flops as shown in Fig. 5. Due to the out-of-plane anisotropies of the free layers, there are two stable magnetization states for each flip flop, which results in four possible magnetization state combinations. Furthermore, the information is always copied from Free Layer 2 (one acting torque) into Free Layer 1 (two acting torques). As shown in Fig. 6 for all four start combinations there is a well defined set of end combinations. These four combinations can be further distinguished into two subsets. For one subset Free Layer 1 and Free Layer 2 possess the same magnetization orientation (Case 1 and Case 4). In these cases neither the torques acting on Free Layer 1 nor the torque acting on Free Layer 2 must change the magnetization states. For the second subset Free Layer 1 and Free Layer 2 exhibit different magnetization orientations (Case 2 and Case 3).

Here, the magnetization orientation encoded spin-transfer torque $\vec{T}_1$ and the auxiliary spin-transfer torque $\vec{T}_{\mathrm{clock}}$ must flip the magnetization state of Free Layer 1 before the spin-transfer torque $\vec{T}_2$ acting on Free Layer 2 destabilized it to a level where read errors occur. Each of these combinations has been mapped to the corresponding starting and ending states under the copy operation and simulated separately (cf. Case 1→Fig. 7,

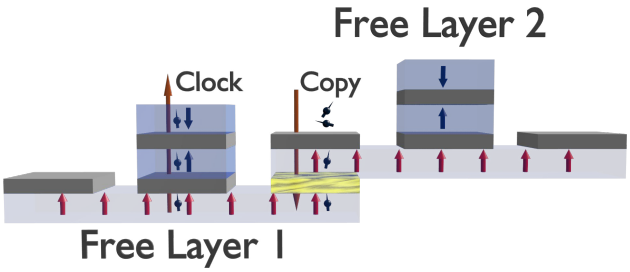

Figure 5: For our study the shift register from Fig. 2 was cut down to two adjacent flip flops. To copy information stored in Free Layer 2 into Free Layer 1 an at first unpolarized current is passed through Free Layer 2, where it gets polarized with the free layers' magnetization orientation and subsequently enters into Free Layer 1, where it exerts a spin-transfer torque which is encoded with the magnetization orientation of Free Layer 2. In order to speed up the switching and prevent the destabilization of Free Layer 2, a second auxiliary spin-transfer torque is acting synchronously on Free Layer 1.

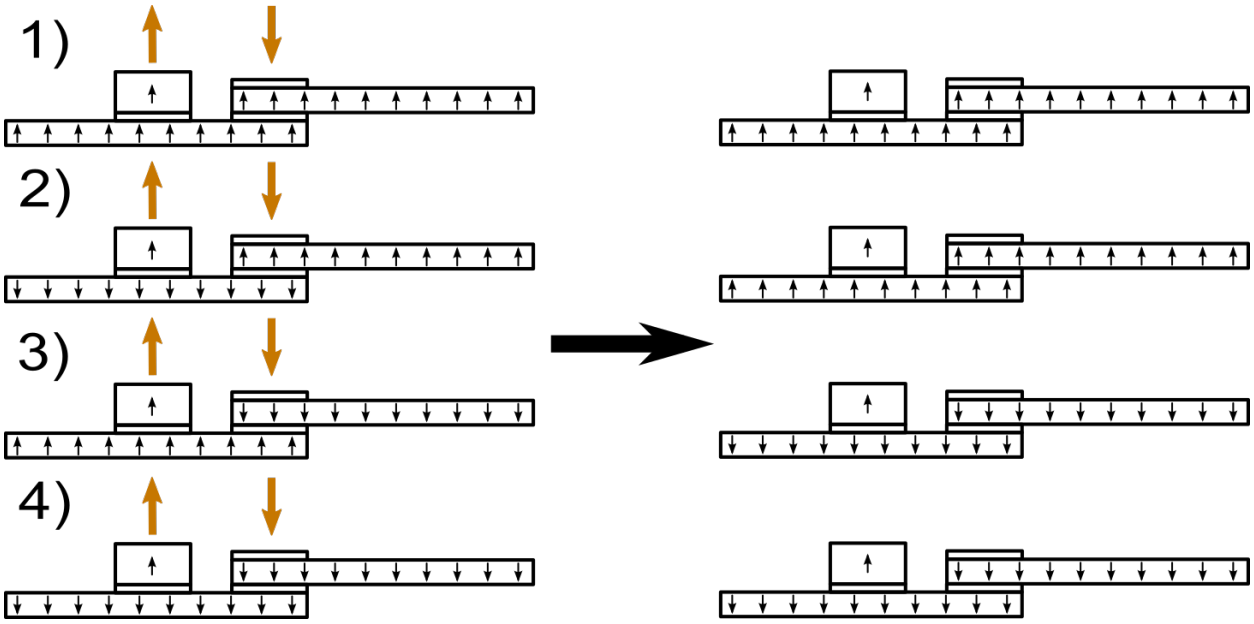

Figure 6: The 2-bit shift register consists of two adjacent free layers which exhibit two stable magnetization orientations. Thus, there are four possible combinations for which the shift register copy operation had to be simulated and analyzed.

Table 1: Simulation parameters

Parameter	Value
Free layer length	120nm
Free layer width	30nm
Free layer thickness	3nm
Contact area	30nm × 30nm
Contact thickness	1.5nm, 3nm, 4.5nm, 6nm
Magnetization saturation M_S	4×10^5A/m
Out-of-plane uni-axial anisotropy K_1	10^5J/m^3
Uniform exchange constant A_{exch}	2×10^{-11}J/m
Polarization P, P_1, P_2	0.3
Non-magnetic layer	Cu
Gilbert gyromagnetic ratio γ	2.211×10^5m/As
Damping constant α	0.01
Non-adiabatic contribution ϵ', ϵ'_1, ϵ'_2	0.1[22]
Fitting parameter Λ, Λ_1, Λ_2	2

Case 2→Fig. 9, Case 3→Fig. 10, and Case 4→Fig. 8). The curves depicted in Fig. 7, Fig. 8, Fig. 9, and Fig. 10 describe the total average of the z-component of the unit magnetization $<m_z>$.

In order to keep the curves in the figures distinguishable only three (#10, #50, and #100) out of the 101 samples are shown. In order to keep the gained results comparable to previously carried out simulation studies, we chose the same parameters as in,[13,13,24] which are summarized in Tab. 1 for the readers' convenience. The free layers for the flip flops have the same size as in[17] (30nm × 120nm × 3nm). The thickness of the interconnecting copper layer has been varied between 1.5nm, 3nm, 4.5nm, and 6nm to change the stray field strength which both free layers experience during the copy operation (see Fig. 5, layer with yellow marble texture). Due to the consideration of thermal excitations, the switching behavior exhibits statistical fluctuations. Therfore, we

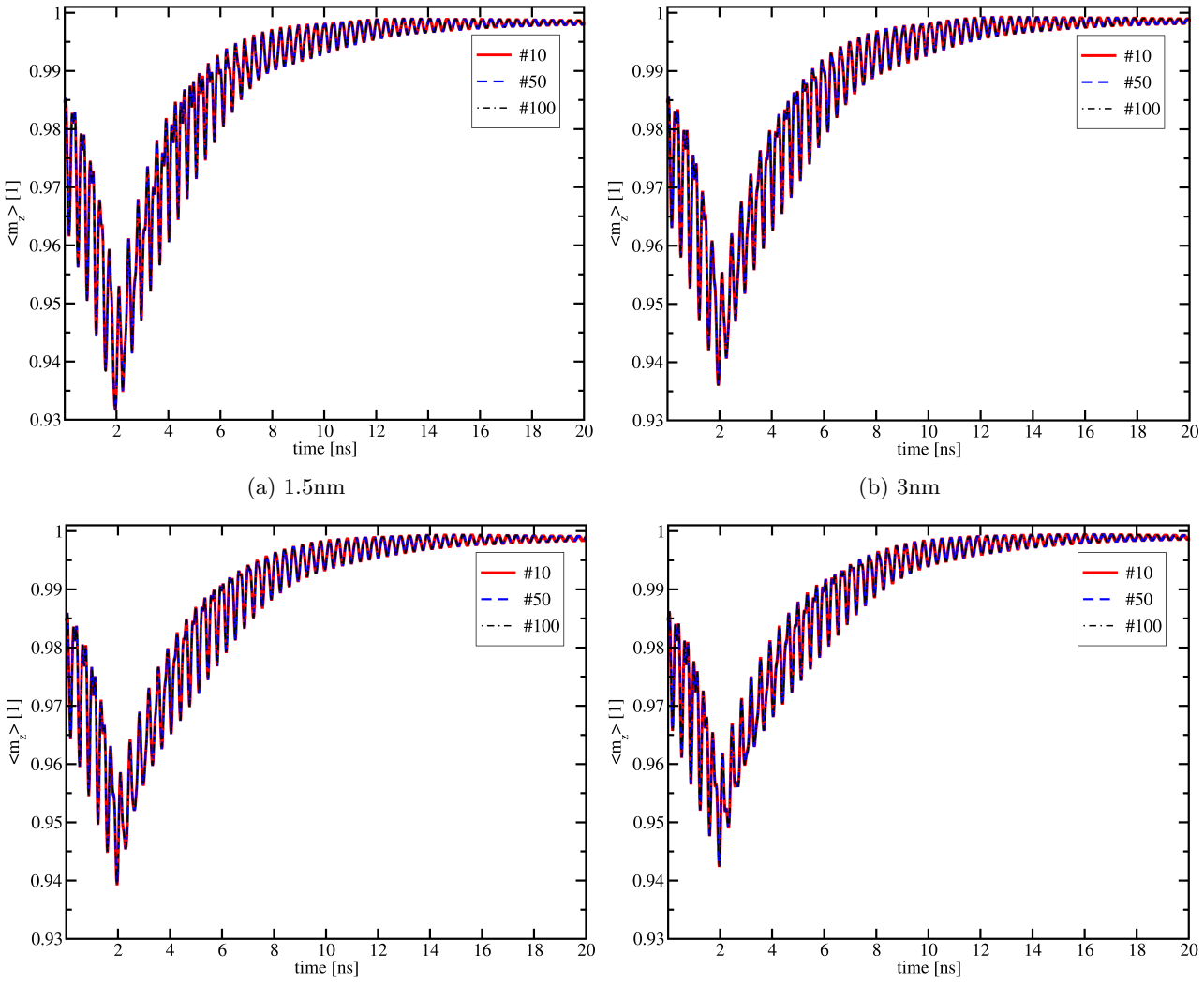

(a) 1.5nm

(b) 3nm

(c) 4.5nm

(d) 6nm

Figure 7: (a), (b), (c), and (d) illustrate the time evolution of the total average unit magnetization $<m_z(t)>$ along the z-axis for the proposed copy operation for Case 1 and an interconnection layer thickness of 1.5nm, 3nm, 4.5nm, and 6nm, respectively (cf. Fig. 6). A small increase in the peak excitation for decreasing interconnection layer thickness (increasing stray field strength) can be observed.

carried out 101 simulations for each combination and thickness to account for possible variations in the switching behavior. Two synchronous 2ns long current pulses with an amplitude of $2 \times 10^{11} \mathrm{A/m}^2$ were applied for the copy operation (positive for copying and negative for the clocked auxiliary torque, as shown in Fig. 5).

4. RESULTS AND DISCUSSION

The first subset of cases (Case 1 and Case 4), where before and after the operation the magnetization states must not change, shows that the pulse length is sufficiently short to prevent an undesired switching event (see Fig. 7 and Fig. 8). Taking a closer look at the figures Fig. 7a, Fig. 7b, Fig. 7c, and Fig. 7d reveals that for increasing interconnection layer thickness the peak of the excitation slightly decreases. On the other hand Fig. 8a, Fig. 8b, Fig. 8c, and Fig. 8d illustrate an even less pronounced excitation with a very small trend towards increasing excitations for bigger interconnection layer thicknesses. We attribute this effect to the difference in the torque

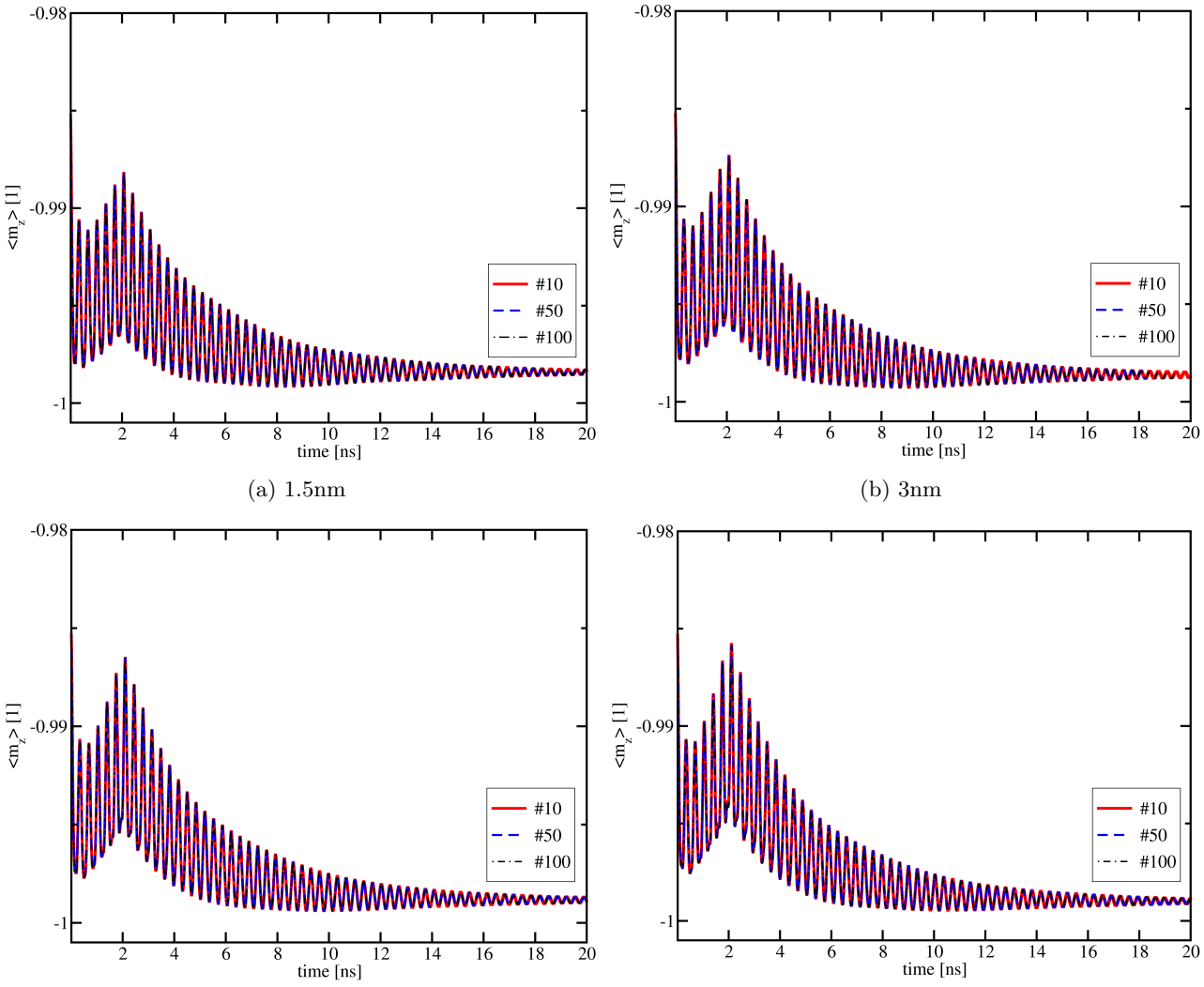

(a) 1.5nm

(b) 3nm

(c) 4.5nm

(d) 6nm

Figure 8: (a), (b), (c), and (d) illustrate the time evolution of the total average unit magnetization $<m_z(t)>$ along the z-axis for the proposed copy operation for Case 4 and an interconnection layer thickness of 1.5nm, 3nm, 4.5nm, and 6nm, respectively (cf. Fig. 6). Only a very small increase in the peak excitation for increasing interconnection layer thickness (decreasing stray field strength) can be observed.

direction for the current flow relative to the magnetization orientation. While for Case 1 the stray field coupling and the spin-transfer torque enforce each other, in Case 4 they counter act each other and damp the precessions.

For the second subset (Case 2 and Case 3), where before the copy operation the magnetization states of the free layers are anti-parallel, only for a interconnection layer thickness of 1.5nm and 3nm the copy operation works flawlessly, while for a thickness of 4.5nm and 6nm the copy operation does not work at all. In comparison to Case 1 and Case 4 the total average unit magnetization $<m_z>$ for Case 2 and Case 3 start at zero. This stems from the fact that the contributions from Free Layer 1 and Free Layer 2 exactly balance each other. However, when the information from Free Layer 2 is copied into Free Layer 1 the total averaged unit magnetization $<m_z>$ must converge towards 1 for Case 2 and towards -1 for Case 3. For Case 2 reducing the interconnection layer thickness from 3nm (Fig. 9b) to 1.5nm (Fig. 9a) leads to a 23% reduction in switching time as well as a 60 times reduction in the standard deviation of the switching time (from $7.21\text{ns} \pm 0.61\text{ns}$ to $5.55\text{ns} \pm 0.01\text{ns}$). Looking at Fig. 9c and Fig. 9d does not show a degradation in the average switching time and distribution - as one would

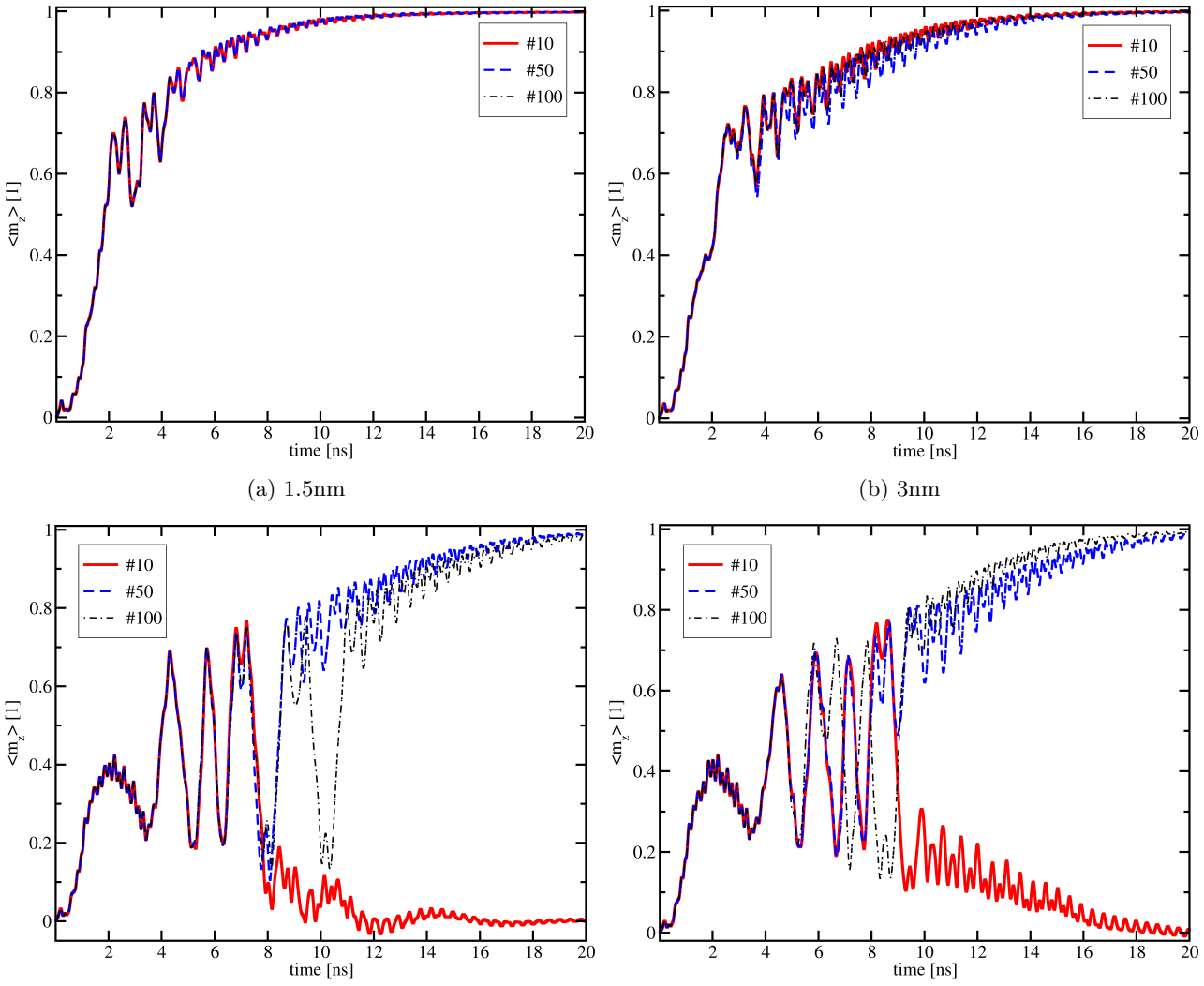

(a) 1.5nm

(b) 3nm

(c) 4.5nm

(d) 6nm

Figure 9: (a), (b), (c), and (d) illustrate the time evolution of the total average unit magnetization $<m_z(t)>$ along the z-axis for the proposed copy operation when considering Case 2 and an interconnection layer thickness of 1.5nm, 3nm, 4.5nm, and 6nm, respectively (cf. Fig. 6). Decreasing the interconnection layer thickness changes the behavior significantly from total failure to 100% switching probability.

expect - but instead the total failure of the copy operation. The oscillations in Fig. 9c are due to the formation of an oscillating domain wall, which completely randomizes the final state it will relax into. In parallel the average switching time increases to $12.32\text{ns} \pm 1.26\text{ns}$ and the switching probability drops down to 50.49%. Also Fig. 9d illustrates that for 6nm the switching suffers under such oscillations and the average switching time increases to $14.2\text{ns} \pm 1.65\text{ns}$ at a switching probability of 58.41%.

Analog to Case 2 there is a significant behavioral difference between the interconnection layer thicknesses of 1.5nm (Fig. 10a) and 3nm (Fig. 10b) on one side and 4.5nm (Fig. 10c) and 6nm (Fig. 10d) on the other side. Again the reduction of the interconnection layer thickness from 3nm ($1.42\text{ns} \pm 0.01\text{ns}$) to 1.5nm ($1.34\text{ns} \pm 0.01\text{ns}$) leads to a $\approx 5\%$ improvement in switching time. The copy procedure fails at 4.5nm (Fig. 10c, $17.16\text{ns} \pm 1.29\text{ns}$ at 34.65% switching probability) and 6nm (Fig. 10d, $7.36\text{ns} \pm 0.48\text{ns}$ at 46.5% switching probability). Interestingly, Fig. 10c shows even more pronounced domain wall oscillations, while for Fig. 10d the switching outcome is random without oscillations.

Fig. 11 summarizes our findings in a box plot for an easy overview (Case 2→C2 and Case 3→C3). The appearance of domain wall oscillations during the copy operation can be clearly identified by the jump in the median switching times (> 10ns) as well as the significant widening of their switching time distributions (cf. 4.5nm C2 and C3, 6nm C2). However, the observed failure mode without the switching time prolonging domain wall oscillations for 6nm interconnection thickness and Case 3 exhibits a very similar switching time and distribution to the 3nm interconnection layer thickness for Case 2. Thus, for mid range switching times with moderate switching distribution widths the information from the box plot is not sufficient as sole reliability check and the actual switching probability must be consulted to determine the reliability.

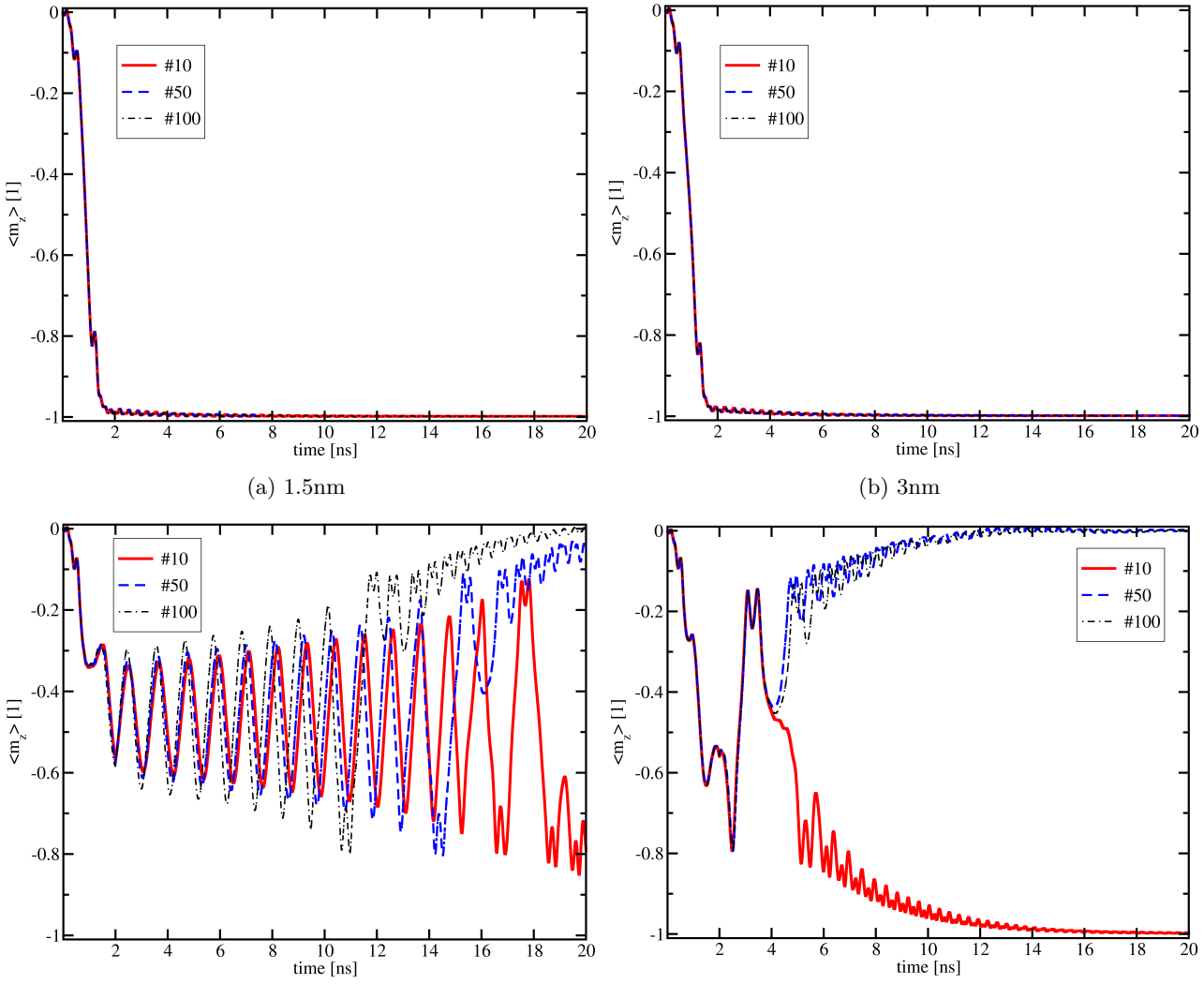

(a) 1.5nm

(b) 3nm

(c) 4.5nm

(d) 6nm

Figure 10: (a), (b), (c), and (d) illustrate the time evolution of the total average unit magnetization $<m_z(t)>$ along the z-axis for the proposed copy operation when considering Case 3 and an interconnection layer thickness of 1.5nm, 3nm, 4.5nm, and 6nm, respectively (cf. Fig. 6). Analog to Fig. 9, a decrease in the interconnection layer thickness changes the behavior drastically from total failure to 100% switching probability.

Since all parameters were fixed and only the distance between the free layers was changed, we attribute the sharp transition between the fully operational regime at 1.5nm and 3nm and the failing regime at 4.5nm and 6nm to the change in stray field strength. This is further supported by the strongly non-linear field strength dependence on the distance $\propto 1/r^3$, e.g. doubling the distance will reduce the field strength to one eighth.

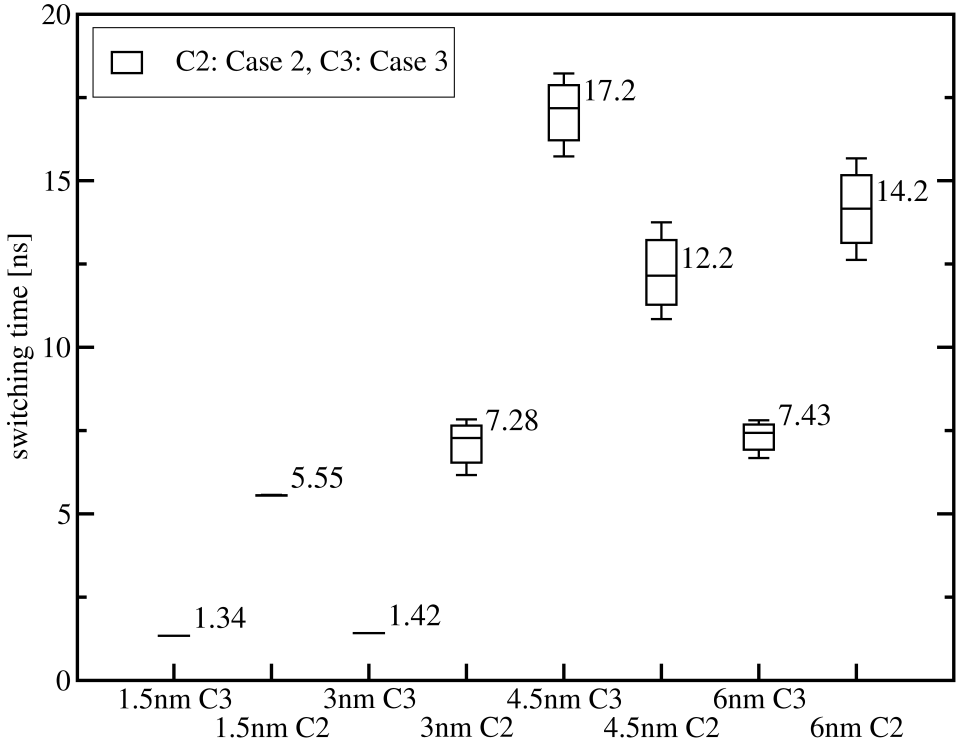

Figure 11: The observed switching times and their distribution in relation to Case 2 and Case 3 as well as the different interconnection layer thicknesses.

Therefore, the much more pronounced stray fields for the closer free layer positions, energetically favor parallel orientations between Free Layer 1 and Free Layer 2 during the copy procedure, while for weak or negligible stray fields the two magnetization states are more or less equal, which allows small (thermal) disturbances to define in which state it will relax into.

5. CONCLUSION

It was shown that the stray field strength has a significant influence on the feasibility of the proposed copy operation. For the studied 2-bit shift register the thickness of the interconnection layer was varied between 1.5nm, 3nm, 4.5nm, and 6nm. For the cases of initially parallel magnetization states of the two free layers before the proposed copy operation, no undesired switching events were observed. However, for initially anti-parallel magnetization states, there is a sharp distinction between structures with close free layers (1.5nm and 3nm distance) and more distant free layers (4.5nm and 6nm). While for close free layers the copy operation is 100% reliable and tends to improve for the smaller distances, the structures with more distant free layers experience domain wall formation and oscillations during switching, which results in reliability problems. We attribute this behavior to the strongly non-linear stray field dependence with respect to distance ($\propto 1/r^3$) and the resulting energetically more favorable parallel relaxation of the magnetization states of the free layers for small free layer distances.

ACKNOWLEDGMENTS

This work is supported by the European Research Council through the grant #692653 NOVOFLOP.

REFERENCES

[1] Zhao, W., Torres, L., Guillemenet, Y., Cargnini, L. V., Lakys, Y., Klein, J.-O., Ravelosona, D., Sassatelli, G., and Chappert, C., "Design of MRAM based logic circuits and its applications," in [*Proc. ACM Great Lakes Symposium on VLSI*], 431–436 (2011).

[2] Marculescu, R., Ogras, U. Y., Peh, L. S., Jerger, N. E., and Hoskote, Y., "Outstanding research problems in NoC design: System, microarchitecture, and circuit perspectives," *IEEE Trans.Computer-Aided Design of Integrated Circuits and Systems* **28**(1), 3–21 (2009).

[3] Nikonov, D. and Young, I., "Overview of beyond-CMOS devices and a uniform methodology for their benchmarking," *Proc. IEEE* **101**(12), 2498–2533 (2013).
[4] Zhao, W. and Prenat, G., [*Spintronics-based Computing*], Springer International Publishing, Cham (2015).
[5] Everspin Technologies. http://www.everspin.com/pub (2016).
[6] Zhang, Y., Zhao, W., Kang, W., Deng, E., Klein, J.-O., and Revelosona, D., [*Current-Induced Magnetic Switching for High-Performance Computing*], 1–51, Springer International Publishing, Cham (2015).
[7] Deng, E., Zhang, Y., Kang, W., Dieny, B., Klein, J.-O., Prenat, G., and Zhao, W., "Synchronous 8-bit non-volatile full-adder based on spin transfer torque magnetic tunnel junction," *IEEE Trans.Circuits and Systems–I: Fundamental Theory and Applications* **62**(7), 1757–1765 (2015).
[8] Deng, E., Kang, W., Zhang, Y., Klein, J.-O., Chappert, C., and Zhao, W., "Design optimization and analysis of multicontext STT-MTJ/CMOS logic circuits," *IEEE Trans. Nanotechnology* **14**(1), 169–177 (2015).
[9] Fong, X., Kim, Y., Venkatesan, R., Choday, S. H., Raghunathan, A., and Roy, K., "Spin-transfer torque memories: Devices, circuits, and systems," *Proc. IEEE* **104**(7), 1449–1488 (2016).
[10] Ikeda, S., Hayakawa, J., Ashizawa, Y., Lee, Y. M., Miura, K., Hasegawa, H., Tsunoda, M., Matsukura, F., and Ohno, H., "Tunnel magnetoresistance of 604% at 300K by suppression of Ta diffusion in $CoFeB/MgO/CoFeB$ pseudo-spin-valves annealed at high temperature," *Appl.Phys.Lett.* **93**(8) (2008).
[11] Chabi, D., Zhao, W., Deng, E., Zhang, Y., Romdhane, N. B., Klein, J. O., and Chappert, C., "Ultra low power magnetic flip-flop based on checkpointing/power gating and self-enable mechanisms," *IEEE Trans.Circuits and Systems–I: Fundamental Theory and Applications* **61**(6), 1755–1765 (2014).
[12] Windbacher, T., Mahmoudi, H., Sverdlov, V., and Selberherr, S., "Rigorous simulation study of a novel non-volatile magnetic flip flop," in [*Proc. International Conference on Simulation of Semiconductor Processes and Devices*], 368–371 (2013).
[13] Windbacher, T., Makarov, A., Mahmoudi, H., Sverdlov, V., and Selberherr, S., "Novel bias-field-free spin transfer oscillator," *Journal of Applied Physics* **115**(17), 17C901–1–17C901–3 (2014).
[14] Windbacher, T., Mahmoudi, H., Sverdlov, V., and Selberherr, S., "Spin torque magnetic integrated circuit." filed: 27.3.2013, EP2784020 (granted April 2016).
[15] Windbacher, T., Makarov, A., Sverdlov, V., and Selberherr, S., "Novel buffered magnetic logic gate grid," in [*Silicon Compatible Materials, and Technologies for Advanced Integrated Processes, Circuits and Emerging Applications 5*], Roozeboom, F., Narayanan, V., Kakushima, K., Timans, P., Gusev, E., Karim, Z., and DeGendt, S., eds., 295–303, The Electrochemical Society (2015).
[16] Windbacher, T., Mahmoudi, H., Sverdlov, V., and Selberherr, S., "Novel MTJ-based shift register for non-volatile logic applications," in [*Proc. IEEE/ACM International Symposium on Nanoscale Architectures*], (2013).
[17] Windbacher, T., Makarov, A., Sverdlov, V., and Selberherr, S., "The exploitation of magnetization orientation encoded spin-transfer torque for an ultra dense non-volatile magnetic shift register," in [*Proc. 46th European Solid State Device Research Conference*], (2016).
[18] Gilbert, T., "A Lagrangian formulation of the gyromagnetic equation of the magnetization field.," *Phys. Rev.* **100**, 1243 (1955).
[19] Kronmüller, H., [*Handbook of Magnetism and Advanced Magnetic Materials*], ch. General Micromagnetic Theory, John Wiley & Sons, Ltd (2007).
[20] Miltat, J. E. and Donahue, M. J., [*Handbook of Magnetism and Advanced Magnetic Materials*], ch. Numerical Micromagnetics: Finite Difference Methods, John Wiley & Sons, Ltd (2007).
[21] Xiao, J., Zangwill, A., and Stiles, M. D., "Boltzmann test of Slonczewski's theory of spin-transfer torque," *Phys. Rev. B* **70**, 172405 (2004).
[22] Khvalkovskiy, A. V., Zvezdin, K. A., Gorbunov, Y. V., Cros, V., Grollier, J., Fert, A., and Zvezdin, A. K., "High domain wall velocities due to spin currents perpendicular to the plane," *Physical Review Letters* **102**, 067206 (2009).
[23] Moriyama, T., Finocchio, G., Carpentieri, M., Azzerboni, B., Ralph, D. C., and Buhrman, R. A., "Phase locking and frequency doubling in spin-transfer-torque oscillators with two coupled free layers," *Physical Review B* **86**, 060411 (2012).
[24] Windbacher, T., Makarov, A., Sverdlov, V., and Selberherr, S., "Influence of magnetization variations in the free layer on a non-volatile magnetic flip flop," *Solid-State Electron.* **108**, 2–7 (2015).